ESA Contract n. 4000132611/20/NL/CRS

Preparation of enabling space technologies and building blocks

GNC and Robotic Arm Combined Control

ESR: Executive Summary Report

Document: ESR_4000132611_20220621

Date: June 21, 2022

Version: 2.0

Prepared by:	Federico Basana	UNIPD-CISAS
Contribution by:	Francesco Branz	UNIPD-CISAS
	Roberto Opromolla	UNINA-DII
	Alessia Nocerino	UNINA-DII
	Claudio Vela	UNINA-DII
	Mauro Massari	POLIMI-DAER
	Davide Invernizzi	POLIMI-DAER
Verified by:	Alessandro Francesconi	UNIPD-CISAS

Table of Contents

Change log

Version	Changes
1.0	*first release*
2.0	Minor changes following RIDs of AR

1 Introduction

The interest in space missions involving Close-Proximity Operations between two satellites and capture of a target object is growing worldwide. For instance, In-Orbit Servicing (IOS) missions have shown their potentialities in extending the operational life of satellites and Active Debris Removal (ADR) missions have been considered necessary to effectively tackle the space debris problem. The IOS missions aim to perform space operation such as up-close inspection, refuelling, repairing and upgrading of another resident space object. In this fashion, the return of investment of a mission can be increased by extending the life of the existing space assets. Moreover, for the capacity of prolonging the operational life of a resident satellite, IOS also represent a solution to mitigate the space debris problem. For what concerns the space debris problem, ADR missions offers the possibility reduce the risk of triggering the Kessler syndrome while freeing usable orbital spots.

The majority of the solutions proposed to safely capture orbital objects relies on robotic systems. Among all, one of the most prominent solutions to the problem is to employ an autonomous spacecraft (chaser) equipped with a highly dexterous robotic arm able to perform the berthing with a resident space object. The technical challenges involved in this operation are complex and span from the approach phase to the after-contact operations. To address these complex challenges, an effective and reliable Guidance, Navigation and Control (GNC) system is of key importance. The European Space Agency (ESA), in cooperation with other space agencies and universities, has been developing technologies in this field for decades.

2 Study objectives

This work presents the results of a research activity performed by a consortium of italian universities under contract with ESA. The study has two objectives: (1) to design navigation and control algorithms of a GNC system for combined control of an autonomous spacecraft equipped with a redundant manipulator with the aim of capturing a target spacecraft; (2) to develop a complete simulation environment used to support the design and testing of the GNC system.

3 Scenarios definitions

An IOS/ADR mission typically involves a chaser spacecraft which needs to approach and perform operations on a target spacecraft. These missions usually consist of several phases; this study focuses on two of them: the reach and capture and the target stabilization phase. In the former the GNC system guides the chaser close to the target through a rendezvous manoeuvre, then the robotic arm is manoeuvred in order to grasp the target. In the latter the chaser consolidates the stack by rigidizing the joints of the robotic arm and eventually executing a manoeuvre to align the centre of mass of the two satellites. For both the considered phases the degree of cooperation and collaboration of the target strongly affects the design of the navigation and control subsystems. The definitions of the cooperativeness and collaboration of the target are reported in Table 1.

The developed GNC system has been tested in three different scenarios. These are reported in

Table 2. The first scenario (SC1) represents an IOS mission in GEO, the target (a large GEO platform) is assumed to be operative, controllable and capable to receive a refuel/update/repair by the servicing satellite; it is considered semi-collaborative and semi-cooperative. The second one (SC2) represents a servicing mission in LEO. In this scenario, the target (Arrow platform - OneWeb) is considered prepared for servicing: it is equipped with a grapple fixture and fiducial markers across the spacecraft body to aid the navigation function. The target is considered non-collaborative during the mission phase and it spins with an angular velocity of 2.5 deg/s. In the last one the capture of a large space debris (ENVISAT) is considered. The chaser is synchronized with the motion of the non-cooperative target which is considered spinning at a rate of 5 deg/s.

Table 1: Definition of collaborativeness and cooperativeness for close-proximity operations

Target Type	Description
Cooperative	The target can provide direct information about its relative states in real-time on-board to the servicer to aid the relative navigation task
Semi-cooperative	The target can provide indirect information about its relative states to the servicer through exploitation of active/passive markers
Non-cooperative	The target does not offer any support for the relative navigation
Collaborative	The target can actively and accurately maintain an attitude profile that can aid the approach and docking/capture process
Semi-collaborative	The target can actively keep an attitude profile to aid the approach but not accurately enough to aid the docking/capture process, i.e., only coarse attitude control is operative
Non-collaborative	The target attitude is uncontrolled and it cannot aid the capture operation in any way

Table 2: Scenarios definition

Scenario	Mission Type	Cooperativeness	Collaborativeness	Target	Orbit
SC1	IOS	Semi-cooperative	Semi-collaborative	SSL-1300 GEO platform	GEO
SC2	IOS	Semi-cooperative	Non-collaborative	Arrow platform (OneWeb)	LEO
SC3	ADR	Non-cooperative	Non-collaborative	ENVISAT	LEO

4 GNC system development

The proposed combined control and relative navigation architectures for the three scenarios are illustrated in this section.

4.1 Relative Navigation Design

A relative navigation solution relying on Electro-Optical (EO) sensors has been selected to provide relative state estimates of the chaser-robotic arm multibody system with respect to the target. One critical design constraint is that the relative navigation function must be able to estimate both the target/chaser (T/C) and the grasping point/end effector (EE) relative states. To this aim, relative navigation is entrusted to two EO sensors rigidly attached to the chaser main body and to the EE. A high-level block diagram of the proposed loosely coupled architecture is provided in Figure 1. Raw EO data are processed to get pose measurements used in the correction step of the filtering schemes. Since the target is a known object, the inputs required by the main processing functions (red) include target, chaser, and robotic arm geometric information (orange), the chaser absolute state estimates and the robotic arm's joint sensors measurements (blue). To allow the G/E relative state estimation filter to operate even in absence of G/E pose estimates, the latter is designed to also receive in input the pose of the EE with respect to the base of the robotic arm (C/E), and the output of the T/C relative state estimation filter. The relative state estimates are fed to the combined control function which provides in feedback chaser commands that can be used by the T/C relative navigation filter to compute the resulting accelerations acting on the chaser.

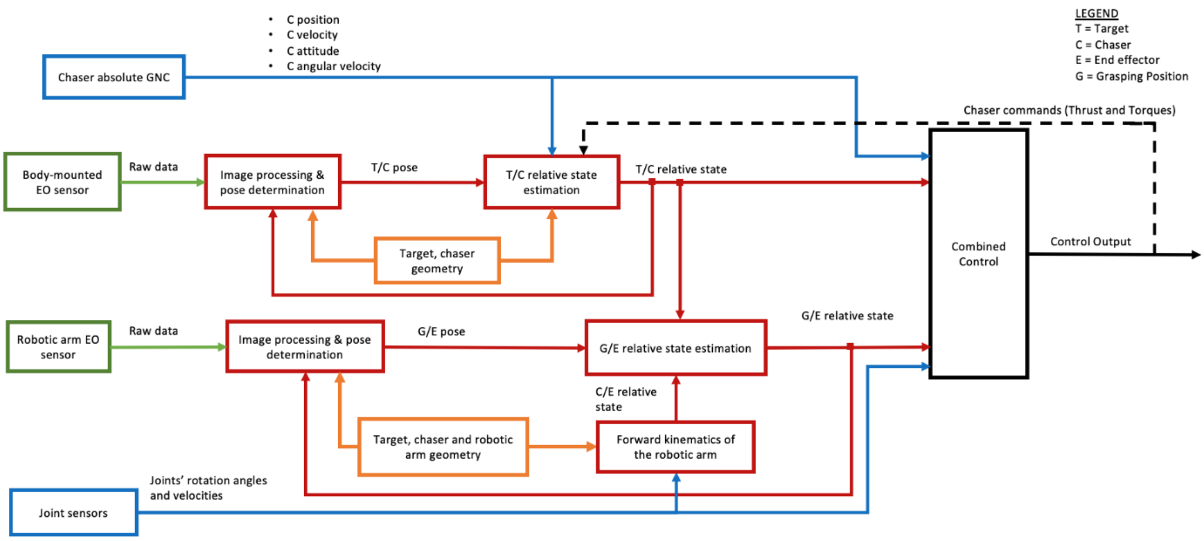

Figure 1: High-level block diagram of the loosely coupled relative navigation architecture developed

A trade-off analysis has been done to carry out the selection of the body-mounted and robotic arm EO sensors, whose result is summarized in Table 3.

Table 3: Sensor selection for the scenarios under study

Scenario	Chaser Body	Robotic arm
SC1	Monocular camera	Monocular camera
SC2	Monocular camera	Monocular camera
SC3	Flash LIDAR	TOF camera

Monocular cameras represent a convenient solution for the semi-cooperative scenarios since the detection and identification of fiducial markers with high angular accuracy allows obtaining highly accurate pose estimates while posing limited constraints in terms of size, weight and power consumption. For SC1, a set of ten retroreflectors illuminated by an infrared laser source on the chaser, is selected as fiducial markers for the body mounted camera. Instead, the robotic arm camera is designed to detect a set of three white circular markers on a black background. For SC2, code-based markers (representing a promising solution for standard-designed targets like the elements of a large LEO constellation) are selected. Specifically, one 20x20 cm^2 AruCo marker is placed at the centre of each target face, while one 5x5 cm^2 AruCo marker is placed

close to the grappling interface.
In both the scenarios, the image processing approach for detection is tailored to the selected markers' typology. Considering that an *a-priori* knowledge of the relative state parameters is available both at the start of the reach and capture phase and at any sub-sequent time frame (as the output of the prediction step of the filters), the identification can be done by reprojecting the markers on the image plane and exploiting the Nearest Neighbour approach. Finally, a non-linear least square PnP solver, based on the Levenberg-Marquardt algorithm, is implemented for pose estimation.

For SC3, the need of direct distance estimates is a critical constraint when dealing with non-cooperative and tumbling targets. Hence, relative navigation is entrusted to active systems producing 3D point clouds from the scene. A high-performance Flash LIDAR is selected as body-mounted sensor while a TOF camera is considered more compatible with the installation constraints on the robotic arm. A customized implementation of the Iterative Closest Point algorithm is selected to provide accurate T/C and G/E pose estimates by registering the measured point cloud to the one obtained by discretizing a CAD model of the target Geometry. Concerning the filtering scheme, a Multiplicative Extended Kalman Filter (MEKF) is selected for both the T/C and G/E relative state estimation tasks in all the scenarios under study. Indeed, this type of filter allows dealing with non-linear systems dynamics, and it is easily implementable. Also, the multiplicative formulation allows avoiding singularities in the covariance matrix due to the unit-norm constraint characterizing quaternion which are used for relative attitude parametrization.

4.2 *Combined Control design*

As a preliminary step to the design of the controller, a rigid multibody model of the system has been developed. Such model includes the chaser platform and a 7 DoF redundant manipulator mounted on the spacecraft base. The equations of motion of the system have been obtained using the floating version of the well-known recursive Newton-Euler algorithm for systems of rigid bodies, which ensure computational efficiency and it allows considering arbitrarily complex configurations. Unlike most of the previous studies in the space robotics field, an orbital disturbance term has been considered in order to evaluate possible undesired effects due to the coupling between multibody and orbital dynamics; this disturbance can be straightforwardly added in the model thanks to the recursive approach. The nonlinear equations of motion of the system can be cast in the following form

$$H(\boldsymbol{q})\begin{bmatrix}\dot{\boldsymbol{\omega}}_b\\ \dot{\boldsymbol{v}}_b\\ \ddot{\boldsymbol{q}}\end{bmatrix}+\boldsymbol{C}(\boldsymbol{\omega}_b,\boldsymbol{v}_b,\dot{\boldsymbol{q}},\boldsymbol{\eta_b},\boldsymbol{r_{b/t}},\boldsymbol{q},t)=\begin{bmatrix}\boldsymbol{M_b}\\ \boldsymbol{F_b}\\ \boldsymbol{\tau}\end{bmatrix}$$

where $\boldsymbol{\omega}_b$, $\boldsymbol{v}_b \in \mathbb{R}^3$are base angular and linear velocity respectively, $\dot{\boldsymbol{q}} \in \mathbb{R}^7$ is the vector of joint angles, $\boldsymbol{\eta_b} \in S^3$ is the unit quaternion describing the base attitude with $S^n = \{v \in \mathbb{R}^{n+1}: \|v\| = 1\}$, $\boldsymbol{r_{b/t}} \in \mathbb{R}^3$ is the position of the base with respect to the target, while $\boldsymbol{M_b}$, $\boldsymbol{F_b}$ $\in \mathbb{R}^3$ and $\boldsymbol{\tau} \in \mathbb{R}^7$ are base torque, force and joint motor torque, respectively. $H \in \mathbb{R}^{13x13}$is the joint space inertia matrix, while $C \in \mathbb{R}^{13}$ is the Coriolis/centrifugal term which accounts for terms related to the relative orbital dynamics.. Concerning the post-capture phase, the target is rigidly attached to the EE. In this case, the stacked configuration (chaser + manipulator + target) can be thought of as a unique multibody system where the last link inherits the inertial parameters of the target. Since in the post-capture phase the position of the base of the stack is not controlled and base body forces are not generated, the system conserves the linear momentum and equation is modified to include the conservation of linear momentum.

As for control design, a combined approach has been proposed wherein base and manipulator states are controlled together. The combined architecture has several advantages over decoupled control strategies, from fuel efficiency to performance improvement.
The proposed control approach consists in using nonlinear controllers whose free parameters (e.g., the PD gains of the feedback part) are tuned by first linearizing the plant and the control law about a reference trajectory and then by leveraging the structured H_∞ framework (see Figure 2). In this manner, it is possible to ensure stability for the nonlinear system while imposing local performance and robustness requirements on the resulting closed-loop about the desired configurations at design time and it is also possible to make assessments on robustness exploiting the structured singular value framework.

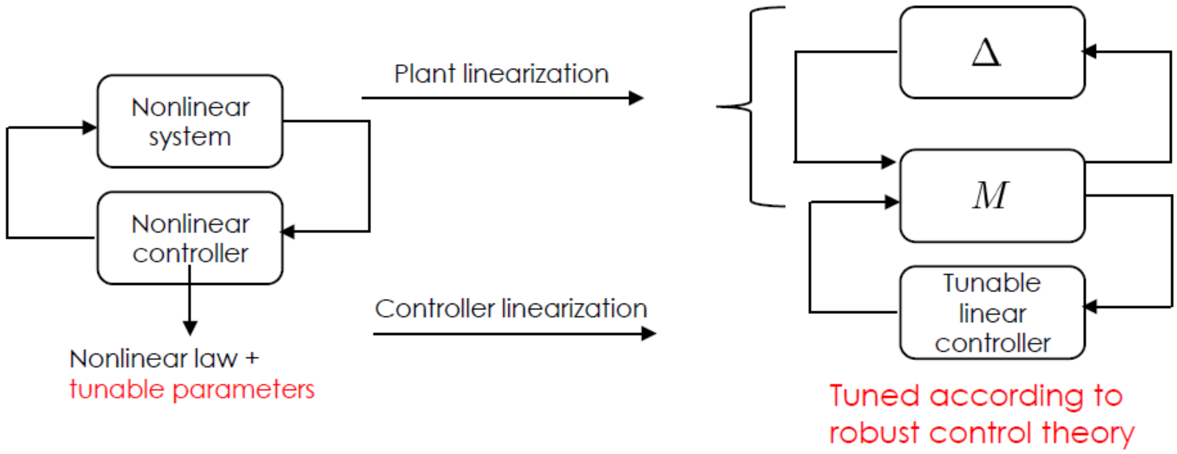

Figure 2 Robustification of nonlinear controllers.

Concerning the control architecture, both joint space and task space controllers have been investigated. The former aims at controlling the joint angles of the manipulator, which are appropriately commanded via the inverse kinematics to track a desired EE pose; the latter directly controls the EE pose.
In both architectures, base pose and generalized velocity feedback are necessary to coordinate base and manipulator control tasks. The controller outputs are the control wrench of the base and the joint torques of the robotic arm. The task space controller has been discarded after a trade-off analysis based on robustness arguments.
The joint space control law is given by

$$\begin{bmatrix} \boldsymbol{M}_b \\ \boldsymbol{F}_b \\ \boldsymbol{\tau} \end{bmatrix} = \widetilde{\boldsymbol{C}}(\boldsymbol{\omega}_b, \boldsymbol{v}_b, \dot{\boldsymbol{q}}, \boldsymbol{q}) + \widetilde{\boldsymbol{H}}(\boldsymbol{q}) \begin{bmatrix} \boldsymbol{a}_\eta \\ \boldsymbol{a}_r \\ \boldsymbol{a}_q \end{bmatrix}$$

where $M_b \in \mathbb{R}^3, F_b \in \mathbb{R}^3, \tau \in \mathbb{R}^7$ are base control moment, force and joint motor torques, respectively, $\widetilde{\boldsymbol{C}}, \widetilde{\boldsymbol{H}}$ are the estimates of Coriolis/centrifugal term and mass matrix, respectively and $\boldsymbol{a}_\eta, \boldsymbol{a}_r, \in \mathbb{R}^3$, $\boldsymbol{a}_q \in \mathbb{R}^7$ are the virtual control inputs based on PD laws.

The control problem has been formulated using the structured H_∞ approach. Simplified performance specifications and control moderation requirements have been imposed by augmenting the plant using frequency weights for the sensitivity and control sensitivity functions. The linearized system has been modelled in Linear Fractional Transformation (LFT) form to account for uncertainties on mass and inertia parameters of chaser and target. In this setting, the controller can be robustly tuned in MATLAB using the advanced methodologies implemented in the *systune* routine. In all cases, the effects of unmodelled phenomena like sloshing and flexibility have been analysed only after control design using μ-analysis.

5 Functional Engineering Simulator

The simulation tool is called Functional Engineering Simulator (FES). It is used to test and validate the developed GNC algorithm. It is implemented in the MATLAB/Simulink environment and makes use of the Simscape Multibody package to represent the dynamics of chaser, target and robotic arm. The simulator reproduces the relative motions of two satellite orbiting the Earth. External perturbations are applied to every component of the system. In addition, nonlinear models are considered in the simulation such as flexibility of structure and sloshing, which can be switched on or off (as the environmental effects) depending on the specific needs of the user. A set of non-linear actuators (MEDs, Thrusters, BLDC motors) and sensors (GNSS receiver, Star Trackers, Inertial Measurements Units IMU, Optical Encoders) models has been developed. The FES is able to simulate the capture phase of different targets in the previously presented scenarios and the dynamics of the stack after the capture. The transition between the two phases is achieved via an analytical formulation, to ensure consistency of the invariant quantities when switching from two independent orbital assets to the stack (unique) configuration. The FES provides 3D visual representations of the scenarios as shown in Figure 3.

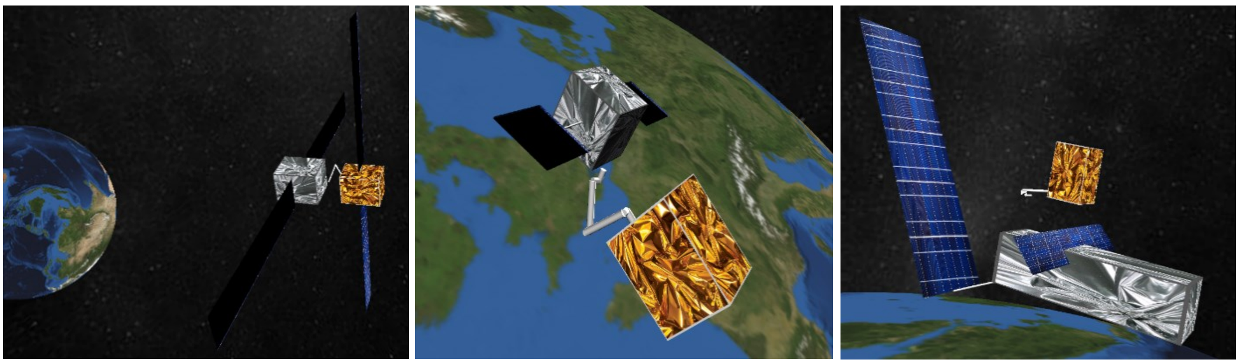

(a) scenario 1 (b) scenario 2 (c) scenario 3

Figure 3: 3D visualization of the scenarios provided by the FES

6 Results

Different analyses have been conducted to validate the developed GNC system and evaluate its performances. Firstly, simulations that considers the real behaviour of actuators and sensors, environmental disturbances and the sloshing of the propellant in the tanks have been executed. Secondly, the error budget analysis has been conducted to identify the major sources of error on the performance of the GNC system. Finally, a Monte Carlo analysis has been done to assess the robustness of the developed GNC system.

6.1 Scenario 1

The characteristics of the target in SC1 (semi-collaborative and semi-cooperative) make this scenario less critical for the developed GNC algorithm, which can grasp the target with a position error norm lower than 5 mm (Figure 4) and an attitude error norm lower than 0.06 deg (Figure 5). In the first 200 s the chaser executes the Reach phase getting to a close distance from the target. In this phase the GNC combined control is not employed and the EE is controlled to keep its velocity equal to zero. The GNC algorithm easily deal with the Stabilization sub-phase despite the large target mass and envelope. However, it has to be considered that in this scenario the target keeps its attitude fixed, helping the GNC algorithm during the robotic arm rigidization.

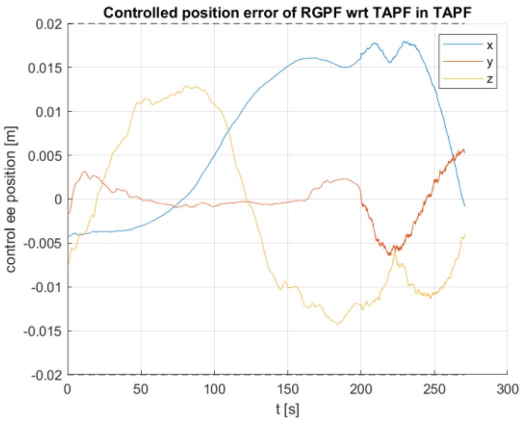

Figure 4: End-effector position control error [m]

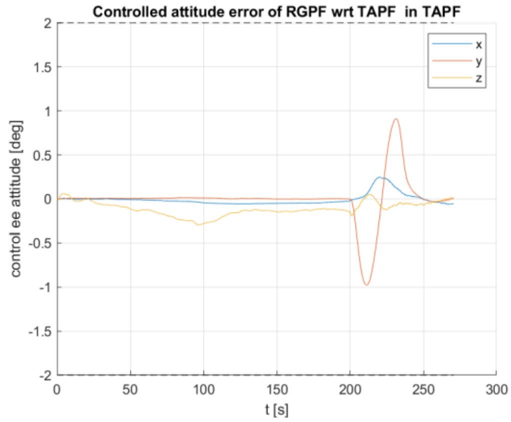

Figure 5: End-effector attitude control error [deg]

6.2 Scenario 2

In scenario 2 the satellite is considered to spin around or the Y axis or the Z axis with an angular rate equal to 2.5 deg/s. This leads to the definition of two different cases for SC2, namely SC2y and SC2z. Since the results are similar only the ones of SC2y are reported. In SC2 the EE successfully grasps the target with a position error norm of about 1 cm (Figure 6) and with an attitude error norm of 0.3 deg. As the error budget analysis confirmed, the oscillatory behaviour is caused by the combined action of the propellant sloshing and the thrusters.

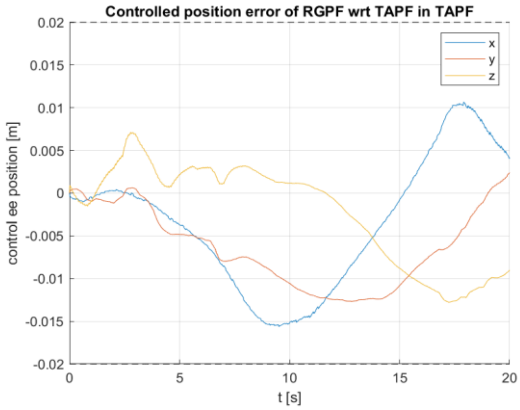

Figure 6: End-effector position control error [m]

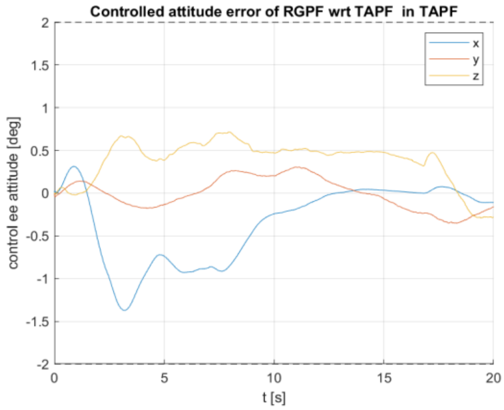

Figure 7: End-effector attitude control error [deg]

6.3 Scenario 3

Scenario 3 is the most challenging for the developed GNC combined control. This is due to the high rotation rate of ENVISAT (5 deg/s): the computation of the target-chaser relative acceleration introduces errors in the GNC system. In addition, the sloshing of the propellant makes this scenario even more challenging. By finely designing the GNC system, the EE grasps the target with a final position error norm lower than 6 cm (Figure 8) and an attitude error norm lower than 0.2 deg (Figure 9).

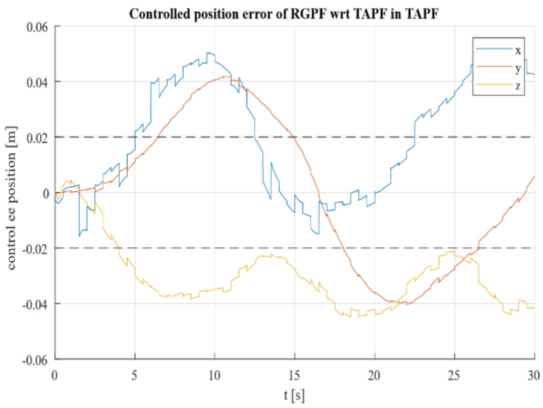

Figure 8: End-effector position control error [m]

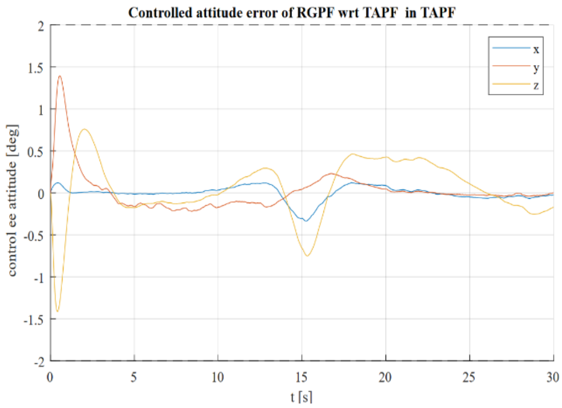

Figure 9: End-effector attitude control error [deg]

6.4 Error Budget and Monte Carlo analyses

An error budget analysis has been conducted in order to identify the major sources of error on the performances of the GNC system. The analysis showed that precise navigation sensors are needed to reduce the error of the state estimation. In addition, the real behaviour of the thrusters introduces errors in all the considered scenarios. The effects of the sloshing of the propellant are visible in scenario 2 and become critical in scenario 3. If the EE performance is considered also the effects of the real BLDC motor and the precision of the encoders of the manipulator joints have to be considered.

A Monte Carlo analysis has been conducted to assess the robustness of the developed GNC system. The mass, the inertia, the Centre of Mass position and the sloshing frequency and damping of the chaser and target have been varied and the performances of the GNC system are evaluated in these non-nominal conditions. The GNC combined control showed good performances in scenario 1 and scenario 2. Scenario 3 confirmed to be the most challenging for the GNC system. At the end of the SC3 Monte Carlo test campaign improvements have been made to assure the robustness of the GNC system in the scenario.

7 Conclusion

The research activity aimed at the development of relative navigation and combined control algorithms for controlling an autonomous spacecraft equipped with a redundant manipulator used to capture a target spacecraft. Numerical testing of the GNC solution proposed was performed through an accurate and realistic simulation tool. The GNC system shows good performance for all the considered scenarios, although SC3 is the most challenging due to the high rotation rate of the target. The error budget analysis has highlighted the major sources of errors. The Monte Carlo analysis quantified the robustness of the GNC system. The developed GNC technology reached a TRL of 4 through to the numerical validation of the alpha version of the GNC code.